ELSEVIER

Polymer 42 (2001) 8241–8248

polymer

www.elsevier.nl/locate/polymer

Small angle X-ray scattering studies on lyocell cellulosic fibres: the effects of drying, re-wetting and changing coagulation temperature

M.E. Vickers[a,*], N.P. Briggs[b], R.N. Ibbett[b], J.J. Payne[b], S.B. Smith[b,1]

[a]*Department of Materials Science and Metallurgy, University of Cambridge, Pembroke Street, Cambridge CB2 3QZ, UK*
[b]*Tencel Limited, 1 Holme Road, Spondon, Derby DE21 5BP (formerly Courtaulds plc), UK*

Received 1 December 2000; received in revised form 6 April 2001; accepted 6 April 2001

Abstract

Lyocell fibres have been characterised by small angle X-ray scattering as-produced wet (never-dry), after drying and after subsequent re-wetting. In all the fibres, the scattering bodies are long and quite well oriented rods or ribbons. The never-dry fibres have the longest (5000 Å) water-filled voids with a cross-sectional correlation length of 30 Å. On drying the scattering bodies become shorter (1600 Å) and the cross-sectional correlation length increases (50 Å) and on re-wetting the voids become much shorter (400 Å) and smaller in cross-section (28 Å). Dry fibres are the most highly oriented (FWHM 13°) followed by never-dry ones (19°) and on re-wetting there is a loss of orientation (24°). Compared to the never-dry fibres re-wet ones show minor differences in the size of the cellulose containing regions (18–22 Å) and a significant decrease in the size of the water containing regions (52–27 Å). Although the wet fibres give good fits to Porod's law, the dry ones do not. The background at higher scattering vectors is relatively high and consistent with scattering from small inhomogeneties or defects. Thus, the wet fibres contain 2 phases, crystalline cellulose and water, and the dry ones 3 phases, crystalline cellulose, large air-filled voids and small defect regions. Increasing the coagulation temperature increases the water content and the size of the water containing regions in all wet samples giving improved dyeablity.

Keywords: Small angle X-ray scattering (SAXS); Cellulose; Voids

1. Introduction

Lyocell is the generic name for cellulosic fibre manufactured by the amine oxide direct dissolution route [1,2]. Only a few specific amine oxides are effective as true solvents and *N*-methyl morpholine *N*-oxide was selected as offering the most attractive process on the basis of process efficiency and chemical availability [3]. The continuous recycling of the solvent means that the chemical operating costs of the direct dissolution process are low, and the lack of an alkali-ripening step means that the molecular weight of the final fibre is higher than achieved in the older carbon disulphide viscose process [4].

In the lyocell process the cellulose raw material is first mixed at elevated temperature with a concentrated solution of the amine oxide. The water content of the mixture is reduced and the amine oxide to water ratio approaches the monohydrate stoichiometry, where the ternary phase diagram exhibits a homogeneous region. The resulting highly viscous solution is extruded at high temperature through an array of spinneret holes, and the solution filaments are then accelerated under tension through an air gap. The cellulose relaxation slows and the polymer chains are aligned in the filament direction. This molecular orientation is fixed by precipitation of the cellulose in a dilute aqueous bath. A bi-continuous texture is formed, consisting of orientated domains of cellulose interspaced by the dilute solution phase, which is considered to be consistent with the mechanism of spinodal decomposition. The cellulose phase then coalesces further during washing [5] and the removal of the water phase by drying leads to the full dehydration of the cellulose domains. The interconnected structure collapses and organises to form the recognisable crystalline morphology of the final fibre [5–8]. This structure means that the fibre has a high initial modulus and a high breaking stress compared to cellulosics manufactured using the viscose process [5].

The final dried lyocell fibre can be accessed by water or other hydrophilic reagents, resulting in the formation

* Corresponding author. Fax: +44-1223-334567.
E-mail address: mev20@cam.ac.uk (M.E. Vickers).
[1] Current address: Hexcel Corporation, 3300 Mallard Fox Drive, Decatur, Alabama 35609, USA.

0032-3861/01/$ - see front matter
PII: S0032-3861(01)00266-X

of liquid filled spaces between the oriented cellulose domains [9–11]. The expansion in the fibrillar structure is almost entirely in the lateral dimension, which means that the fibre has high longitudinal stability in the wet state. During reswelling water accesses the non-crystalline regions of the fibrillar structure, which leads to the disruption of cellulose hydrogen bonding and a suppression of the cellulose T_g [6,12]. The initial modulus of the fibre is reduced in the wet state and the extensibility is increased [13].

Many types of fibre give small angle X-ray scattering (SAXS) from oriented inhomogeneities, which are characterised either as crystalline fibrils [14–16] or as voids [17–19]. In general data from other techniques, for example electron microscopy or density, are required to confirm the exact nature of the scattering bodies. Some systems may even be characterised on the basis of three distinct phases, which complicates the interpretation further. In the dry state the SAXS of cellulosic fibres is concentrated at low scattering vectors, and it spreads to higher values when swelling occurs in water [13,14]. Crawshaw and Cameron [20] used in-situ SAXS to study repeated drying and re-wetting of lyocell cellulosic fibres, finding that in the dry state the void fraction decreased but the average void length and void cross-sectional size increased. The repeated treatments reduced the wet volume fraction of the voids and their length but not the cross-sectional size. This was suggested to be due the formation of additional hydrogen bonding between the fibrillar domains, which inhibited the expansion of pore spaces on rewetting. Small angle neutron scattering [21] has been used to confirm that scattering in these wet fibres comes from contrast between crystalline cellulose and water and that any possible scattering from dry voids or non-crystalline regions is within experimental error.

Some wet spun fibres have been examined in, or near to their, original as-formed wet state structure: for Poly[p-phenylene(benzo[1,2-d:4,5-d′]bisthiazole-2,6-diyl)] (PBT) resin was used to minimise changes on drying [22], and for poly(p-pheynlene terephthalamide) (PPTA) drying was done in critical-point carbon dioxide [23]. The PPTA results were consistent with spinodal decomposition and then crystallisation occuring during coagulation.

The work reported in this paper was aimed at investigating the structures that cause the observed SAXS of lyocell, and the textural changes that occur when as-spun fibres are dried and re-wetted. The effect of changes in the fibre coagulation temperature has also been studied, in order to learn more about the phase separation mechanism [24]. A better understanding of the development and structure of the fibrillar morphology of lyocell should provide important insights into the observed mechanical and hydration properties of the fibre. The manipulation of texture development during spinning and coagulation may provide methods of controlling the final mechanical and physical properties of the fibre, so allowing its use to be optimised for different applications [24].

2. Theory

Without making any assumptions about the type of structure, a few parameters can be obtained from SAXS data to characterise two-phase heterogeneous systems [18,22,23,25,26]. The formulae for unoriented systems can be modified for oriented systems to give information about the structure perpendicular to the fibre axis.

With intensity $I =$ intensity for slit-smeared equatorial data from a cylindrically oriented sample (or meridionally averaged two-dimensional data), the scattering vector $s = 2\sin\theta/\lambda$, $\theta =$ half the angle through which the beam is scattered and $\lambda =$ wavelength, the invariant, integrated intensity (used for scaling) is

$$Q = \int_0^\infty sI(s)\,\mathrm{d}s \tag{1}$$

and the Porod constant is

$$K_p = \lim_{s\to\infty} s^3\, I(s) - I_{bg} \tag{2}$$

This assumes that the boundaries between two phases are sharp (on a scale 2–15 Å) and that the background scattering is independent of scattering vector, which implies that it is a simple two phase system with no significant electron density variation in either phase. The correlation length is

$$L_c = 1/\pi \int_0^\infty I(s)\,\mathrm{d}s/Q \tag{3}$$

and the Porod length is

$$K_p = Q/(2\pi_{Kp}) \tag{4}$$

With a measurement of the volume fractions of each phase (Vf_1 and Vf_2) this weighted average can be separated into two Porod lengths

$$L_p = L_{p1}Vf_2 = L_{p2}Vf_1 \text{ also } 1/L_p = 1/L_{p1} + 1/L_{p2} \tag{5}$$

specific length (or surface area)

$$SL = K_p\, Vf_{cel}Vf_{H_2O}2\pi^2/Q \tag{6}$$

Note that all the integrations are strictly from $s = 0$–∞ but data can only be obtained over a limited range. Thus some attempt at extrapolation may be required.

If the interparticle interference can be ignored and the size distribution is narrow, the radius of gyration R_g can be obtained from a Guinier plot at low s [27]

$$R_g^2 = -\ln I/2\pi^2 s^2 \tag{7}$$

For two-dimensional pinhole data, the meridional broadening will contain a component that relates to size broadening (L) and one that relates to orientation (B_ϕ). As these components differ in the way that the broadening varies with scattering vector Ruland [28] has developed a method of separating these two effects

$$s^2B_{obs}^2 = 1/L^2 + s^2B_\phi^2 \quad (8)$$

where B_{obs} is the observed breadth at a given value of s. This assumes that the peak profiles are approximately Gaussian. If they are approximately Lorentzian Eq. (8) takes the form [29]

$$sB_{obs} = 1/L + sB_\phi \quad (9)$$

It is most likely that the peaks will be a mixture of Gaussian and Lorentzian and thus the best result is probably intermediate between that of Eqs. (8) and (9). Also, these equations strictly apply the intergal breadth and not the full width at half maximum although the latter is frequently used. Note that L is a length of coherence along of the fibre axis, to which both phases may contribute.

3. Experimental

Two sets of samples have been examined. The first set was manufactured in a large-scale process and studied as made (never-dry), dry and wet after re-wetting (re-wet). The second set was made in a small-scale laboratory process so that the temperature of the coagulation bath could be varied. Fibre was sampled prior the drying stage (never-dry) from a production line and retained in the wet state before examination in water. This fibre was then dried in ambient conditions to provide dry samples, and re-wet with distilled water to give re-wet samples.

The weight ratio of cellulose to water was obtained by soaking approximately 1 g of fibres in distilled water and removing the excess water by centrifugation. The wet sample was weighed and then dried before reweighing.

Dyeability was determined by comparing the up-take of Solophenyl Green 5BL dye by the sample fibre to that of a standard fibre. The depth of dyeing was measured by a spectrometer, which records the intensity of light across the visible spectrum referenced against a standard white tile.

Dyeability = 100 × (intergrated intensity of sample − that of std)/intergrated intensity of std.

2-D digital X-ray data were collected at Daresbury station 16.1 [30] with a wavelength of 1.41 Å and 3 m from the sample to the area multiwire proportional counter. Small bundles of fibres, giving a cylinder about 2 mm in diameter, were mounted across 35 mm slides and placed vertically in the X-ray beam. Short exposure times were used up to a maximum of 2 min and typically 6 s. Although the wet samples were open to atmosphere during exposure, there was no evidence of the samples drying out. The data were corrected for detector response. An empty mount was used as a blank, negligible background scatter was observed, consequently there was no background subtraction carried out on the data. No correction was made for fluctuations in beam intensity.

Azimuthal scans around the two-dimensional data were extracted at about 10 different values of s and analysed using Eq. (8).

1-D digital data were collected in a step scanning Kratky camera with CuK radiation. To try and optimise the data quality, data were collected in four ranges, with increased step size and dwell time as s increased. The whole run was repeated three times and the data from different runs were averaged. A moving slit device to measure the intensity of the through beam. Samples were examined both dry and wet. The wet samples were held in a 1.5 mm diameter glass capillary and a capillary full of water was used as a blank. Dry samples were taped to a holder, with an empty holder as the blank and examined under vacuum. Extra dry samples were examined sealed in a glass capillary after heating in a vacuum oven.

Data collected in the Kratky camera were processed by scaling to correct for differences in absorption followed by blank subtraction and careful examination to determine the region to use for fitting to determine the Porod constant. The criteria used were (1) intensity approaching low values in a plot of I against s, (2) a straight region with gradient about −3 in the plot of log I against log s and (3) the plateau region beyond the region of steepest ascent in a Porod plot Is^3 against s^3. K_p was determined from a least squares fit of the data to $I(s) = K_p/s^3 + I_{bg}$. After subtracting the constant background from all the data the experimental data (through the fitted region and out to s_{max}) were replaced by the calculated values. In general the backgrounds were low (~0–400 counts/100 s) except for analysis of dry samples (see Section 4).

The data were extrapolated from s_{min} to $s = 0$ by fitting the first five data points to a Gaussian. Most of data processing was carried out using a modified version of Vonk's program [31].

Differences in the low s data, such as the value of s_{min} and the method used for extrapolation, effect the numerator of Eq. (3) and hence the values obtained for the correlation length. Errors in scaling, poor counting statistics, not fitting in the Porod region and insufficient data at higher angles cause errors in the determination of K_p. Errors in determining K_p influence the background, which effects the invariant. However, as the Porod length is determined from a ratio of Q to K_p some of these errors cancel out: repeat runs with rather different amounts of sample in the beam and using different blanks gave large differences in Q and K_p but much smaller differences in L_c (±2 Å) and L_p (±1 Å).

Other parameters were calculated from Q and K_p using Eqs. (5) and (6). The weight ratios of cellulose and water were converted to volume fractions by taking the density of water as 1 and that of crystalline cellulose as 1.6 g cm^{-3}. In

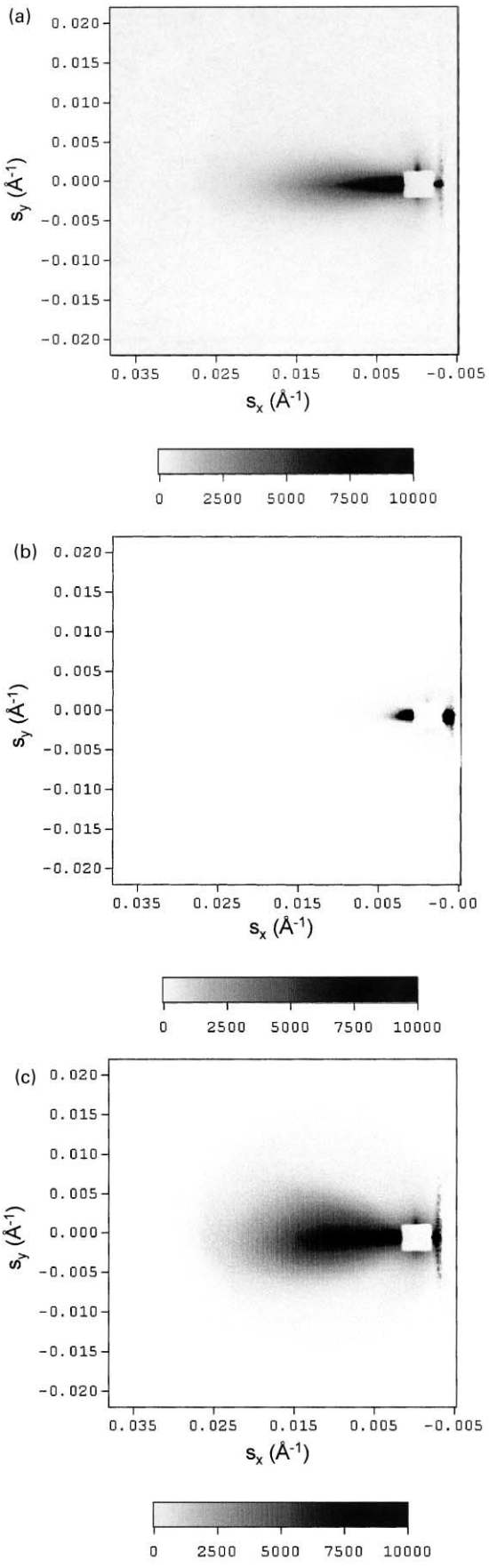

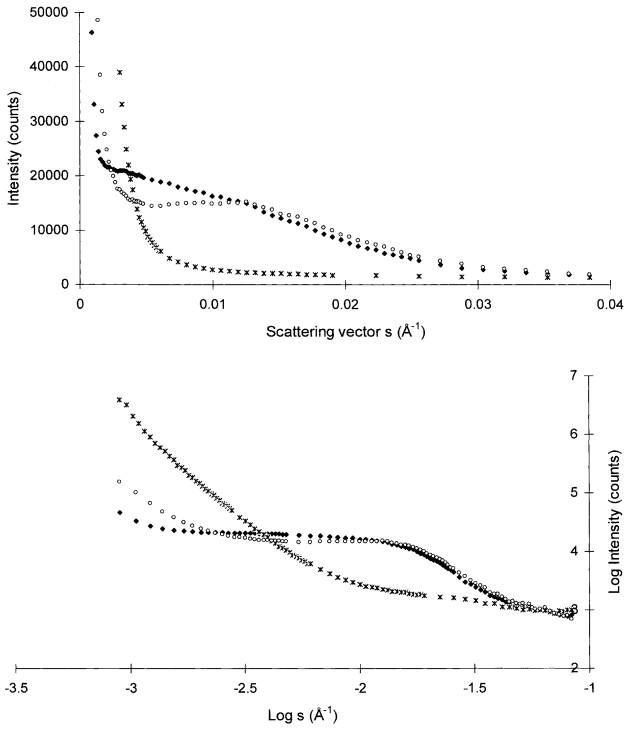

Fig. 2. Kratky SAXS Data (a) linear scales (◆) never-dry, (×) dry and (○) re-wet fibres (b) log scales (◆) never-dry, (×) dry and (○) re-wet fibres.

addition calculations were performed using the experimentally determined density, 1.53 g cm^{-3} for Lyocell fibres.

The dry samples were also analysed by Guinier plots, Eq. (7).

4. Results and discussion

4.1. Large-scale process

Fig. 1(a)–(c) shows the 2-D data with an equatorial streak, which implies scattering bodies that are long in the fibre direction and much smaller perpendicular to it. Differences in the equatorial spread imply that in cross-section the scattering bodies are medium sized when never-dry, increase in size on drying and decrease to a mininium on re-wetting. This can be seen in the Kratky equatorial scans Fig. 2 and these data were used to quantify the differences. The results are shown in Table 1.

The wet samples gave reasonable Porod plots in the region $s = 0.033$–0.40 Å^{-1} ($s^3 = 1.1$–5.8×10^{-5} Å^{-3}), as shown in Fig. 3. In this range on a linear scale the intensity approached background, and on a log–log scale the gradient was about -3.

For the dry samples the situation was more complex. On a linear scale the scattering appeared to approach background

Fig. 1. Two dimensional SAXS Data (a) never-dry (b) dry (c) re-wet.

Table 1
Results from large scale process

	Never-dry	Dry	Re-wet	Dry 2[a]	Dry 3[b]
Correlation length (Å)	30[c]	55[d]	28[c]	64[d]	63[d]
		50[e]		60[e]	59[e]
Porod length (Å)	13[c]	1020[d]	12[c]	842[d]	1170[d]
		75[e]		79[e]	75[e]
Wt Water:cellulose ratio	2.27		0.9		
Vf cellulose	0.22		0.41		
Porod water length (Å)	59		29		
Porod cellulose length (Å)	17		20		
Radius of gyration (Å)		333[f]		312[f]	314[f]
		76[g]		77[g]	78[g]
Average length (Å)	5000	1600	400		
Orientation, FWHM (deg)	19	13	24		

[a] 6 h at 60°C in vacuum oven.
[b] 226 h at 60°C in vacuum oven.
[c] Fitting range for Porod's law, $s = 0.022–0.40$ Å^{-1}.
[d] Fitting range for Porod's law, $s = 0.0068–0.026$ Å^{-1}.
[e] Fitting range for Porod's law, $s = 0.026–0.058$ Å^{-1}.
[f] Fitting range for Guinier, $s = 0.00009–0.00123$ Å^{-1}.
[g] Fitting range for Guinier, $s = 0.0018–0.0037$ Å^{-1}.

at about $s = 0.01–0.02$ Å^{-1} but in this region the log–log plots gave gradients of less than -1. This region can be forced to fit Porod's law with high background scattering such as might come from inhomogeneties in one of the regions. On the log–log plot there appears another increase in the gradient in the range $s = 0.03–0.05$ Å^{-1} and fitting in this range gives a lower background than trying to fit in the range $s = 0.01–0.02$ Å^{-1}. In fact, on the Porod plot several different regions can be found to which Eq. (2) can be applied. Each gives different slopes and intercepts, that are the backgrounds and Porod constants. In the region ($s = 0.0016–0.004$ Å^{-1}) where the log–log gave a gradient of about 3 the scattering was considerably above background. Thus for the dry sample it was not possible to find a range that agreed with all three criteria given earlier.

The correlation lengths obtained were relatively insensitive to the Porod fitting region but the Porod lengths were very sensitive to it. The long weak tail at higher angles probably comes from very small regions of disordered material. To check whether this scattering could come from low levels of water retained in the dry fibre, samples were examined after drying and sealed in a glass capillary. No significant difference was observed between nominally dry samples with different levels of humidity, see Table 1. However, it is possible that samples originally dried at different temperatures may show some structural differences.

For dry fibres Guinier radii of gyration were calculated, see Fig. 4. Curvature of the Guinier plots implies that the bodies are polydisperse and/or anisotropic. Again no difference was observed between samples with different humidity levels. The apparent difference in intensity is probably due to differing amounts of sample in the X-ray beam.

Fig. 5 shows some of the azimuthal scans extracted at different scattering vectors and Fig. 6 the Ruland plot for the never-dry fibre. Results for the average length and orientation are given in Table 1. The peak profiles did not fit any ideal shape but were probably more Lorenztian than Gaussian.

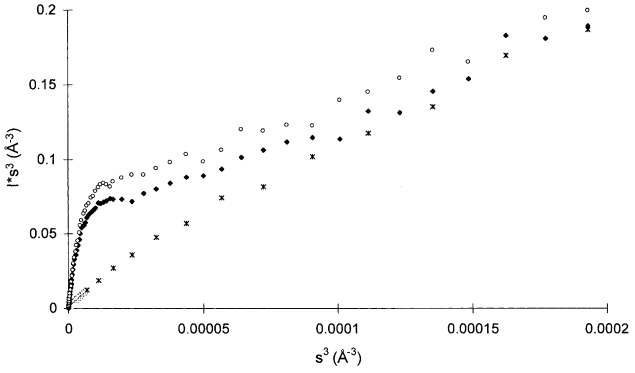

Fig. 3. Porod plots for (◆) never-dry, (×) dry and (○) re-wet fibres.

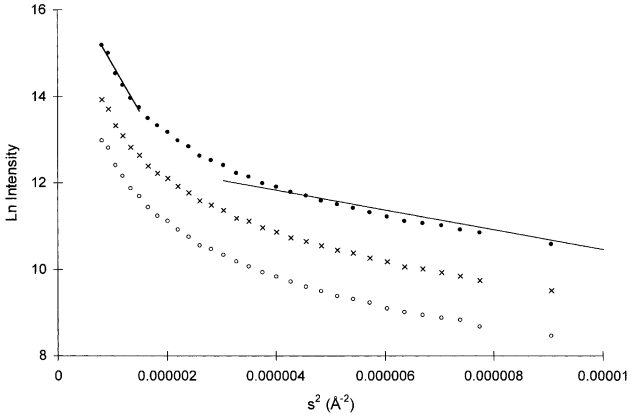

Fig. 4. Guinier plot for dry fibres (●) dried in ambient, (×) dry2 vacuum oven for 6 h, (○) dry3 vacuum oven for 22 h.

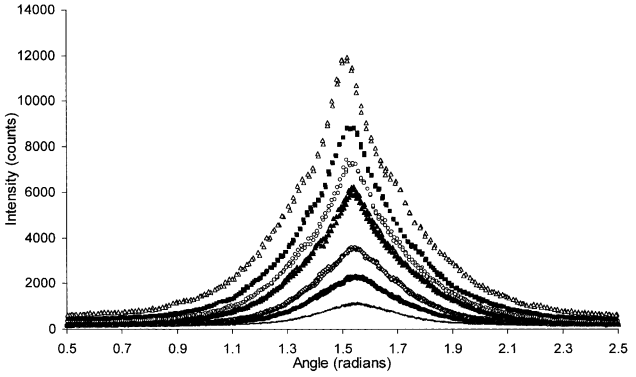

Fig. 5. Azimuthal scans at different vales of s for never-dry sample (Fig. 1a).

Use of Eq. (9) instead of Eq. (8) gives approximately the same orientation but longer bodies. No correction has been made for the size of the X-ray beam, which is about 3 mm in the equatorial and 1 mm in the direction lateral to the fibre axis. The correction would be relatively small and also tend to increase the length. Any of these refinements will alter the actual numbers but not the observed trends.

As all the wet samples gave reasonable Porod plots it is considered that these consist of a two-phase system of crystalline cellulose and water. This has been confirmed by a SANS experiment, [21] which showed that the small angle scattering disappeared near the match point. Use of the experimentally determined density1.53 g cm^3 instead of a crystalline density 1.6 g cm^3 made only a small difference (<2%) to the sizes calculated for cellulose and water regions.

For the dry fibres the situation is more complex. The experimentally measured mass density of the fibres is 1.53 g cm^3 and the crystalline density, from cell parameter measurements, 1.6 g cm^{-3}, which compares favourably with the literature value of 1.61 g cm^{-3} [32]. The reduction in mass density could come from air-filled voids and or non-crystalline material. Wide angle X-ray scattering implies

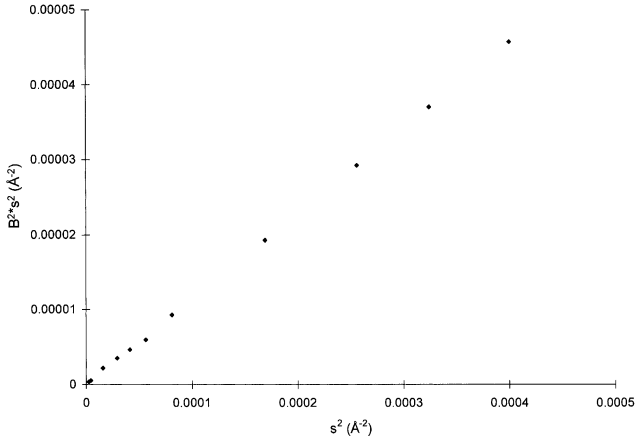

Fig. 6. Ruland plot for never-dry sample.

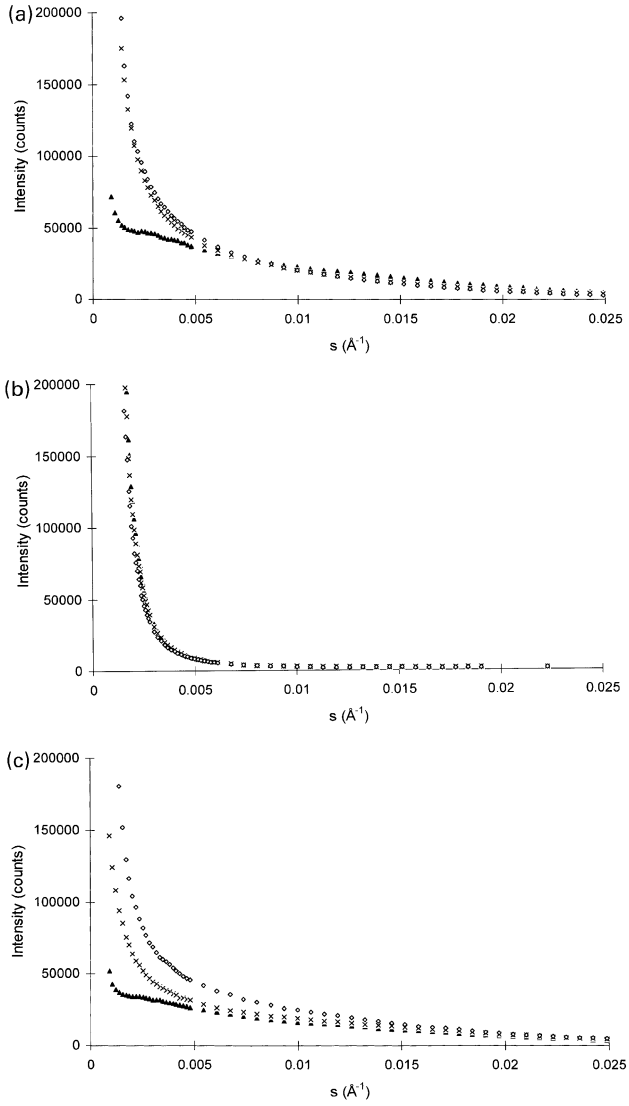

Fig. 7. Kratky SAXS Data for samples coagulated at different temperatures (▲) 22, (×)72, ◇ 97 (a) never-dry, (b) dry, (c) re-wet.

that the fibres are predominately crystalline cellulose with some disorder. The presence and amount of non-crystalline material depends upon assumptions made about the density of any non-crystalline material. Simple profile fitting to the meridional data gives crystallinity ~80–100%. There is no interference peak for the dry fibres, which implies that the scattering bodies are dilute. The model, which currently gives the best agreement with existing experimental data is one in which the bulk of the SAXS comes from larger air-filled voids but there is also a contribution from smaller non-crystalline regions.

It is interesting to note that for the wet samples the ratio of L_c:L_p is about 2. No further comment can be made about the dry fibres because of the difficulties to deciding where to fit Porod's law. L_c is biased towards larger bodies and L_p to smaller ones and so the ratio gives some measure of polydispersity and anisotropy. Janosi's [33]

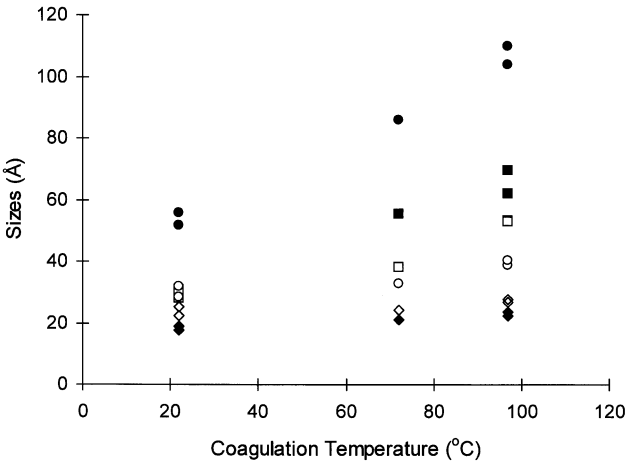

Fig. 8. Influence of coagulation temperature on cross-sectional sizes of wet fibres (■) correlation length never-dry, (□) correlation length re-wet, (◆) Porod cellulose length never-dry, ◇ Porod cellulose length re-wet, (●) Porod water length never-dry, (○) Porod water length re-wet.

calculations show that for a sphere the ratio is 1.125 and for a long rod 1.33. Ruland's work on carbon fibres [18] gave a ratio of about 2. Schurz and co-workers [34] have used this ratio to differentiate between different types of cellulosic fibres. However, there are insufficient experimental details to be able to compare their work to these results.

4.2. Smaller scale process with coagulation at different temperatures

Fig. 7(a)–(c) shows the SAXS data for never-dry, dry and re-wet fibres coagulated at 22, 72 and 97°C. Fig. 8 summarises the results of size changes with different coagulation temperatures. Increasing the coagulation temperature increases the water content and the cross-sectional size of the water-containing region. There are much smaller differences in the sizes of the cellulose regions. Multiple data points are from repeat data collections for samples coagulated at lowest and highest temperatures to give some estimate of repeatability, which is about 5%. The increase

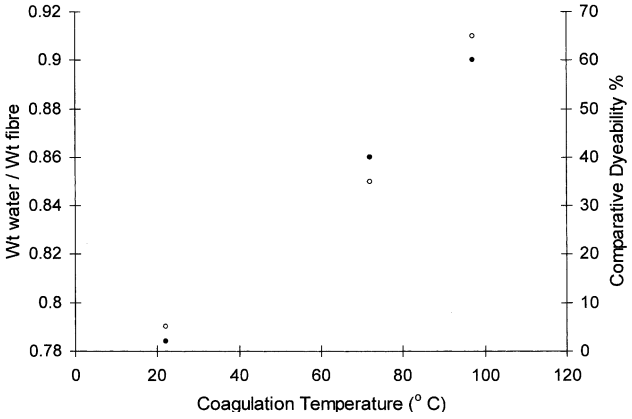

Fig. 9. Influence of coagulation temperature on water content and dyeability, (○) weight of water/weight of fibre, (●) comparative dyeability.

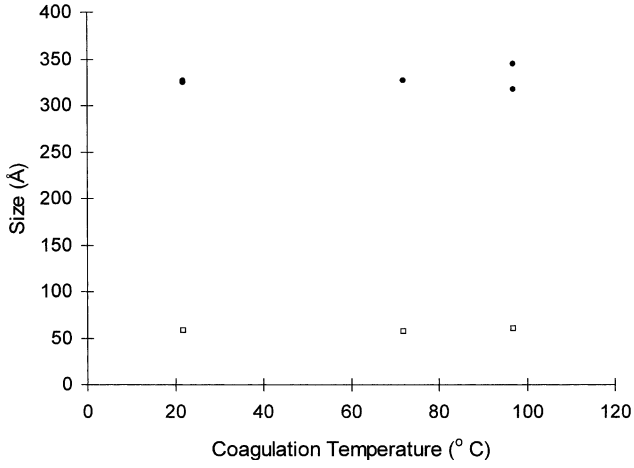

Fig. 10. Influence of coagulation temperature on cross-sectional sizes of dry fibres (□) correlation length, (●) radius of gyration.

in the size of the water containing regions improves dyeability, as shown in Fig. 9. The coagulation temperature appears to have no influence on the size of the voids in dry fibres, see Fig. 10.

As expected, samples from the small-scale process coagulated at 22°C (see Fig. 8) gave similar, but not identical, sizes to those obtained in the large-scale process coagulated at ambient temperature (see Table 1).

5. Conclusions

SAXS data have been used to follow the changes in pore dimensions and orientation on going from never-dry to dry and then re-wet cellulose. The wet fibres are two phase (water and crystalline cellulose) but the dry ones are probably three phase (air, crystalline cellulose and non-crystalline cellulose). The never-dry fibres have long and well-oriented water-filled voids with diameters that are classed as medium sized. In cross-section, the water containing regions are substantially larger than the cellulose ones. On drying many of these voids close up leaving a few relatively large ones, which are well oriented. In addition there are defects in the crystalline regions probably where voids have closed up. On re-wetting the water penetrates into voids and the defect regions. The latter swell and the former shrink to give shorter and less well oriented voids that have a smaller cross-sectional size. Because the water content is reduced the cellulose and water cross-sectional sizes are now approximately similar.

Increasing the coagulation temperature coarsens the structure by increasing the size of the water-filled regions. This is most evident in never-dry samples, is also observed in re-wet samples but is not apparent in dry samples.

Acknowledgements

We would like to thank Dr E Towns-Andrews, Professor

A J Ryan, Dr N J Terrill and Dr J P A Fairclough for help with SAXS experiments at Daresbury, Dr Ruth Cameron and Dr Jane Crawshaw (University of Cambridge) for helpful discussions and Tencel Limited (formerly Courtaulds plc) for permission to publish.

References

[1] Franks NE, Varga JK. US Patent No 4,196, 1 April 1980;282.
[2] Armstrong RN, Varga JK, McCorsley CC. TAPPI Intl Dissolving Pulp Conference Proceedings, 1980. p. 99–104.
[3] Johnson DL. Eastman Kodak Co, Rochester NY, US Patent, 3,447, 3 June 1969;956.
[4] Moncreiff RW. Man-made fibres. 5th ed. Butterworth, 1970 (chap. 2).
[5] Dube M, Blackwell RH. TAPPI Intl Dissolving and Speciality Pulps Conference Proceedings, 1983. p. 111–9.
[6] Lenz J. Appl Polym Sci 1988;35:1987.
[7] Chanzy H, Nawrot S, Peguy A, Smith P. J Polym Sci Polym Phys 1982;20:1909.
[8] Heikens D, Hermans PH, Van Velden PF, Weidinger A. J Polym Sci 1953;XI:433.
[9] Lenz J, Schurz J, Wrentschur E. Acta Polym 1982;43:307.
[10] Morton WE, Hearle JWS. Physical properties of textile fibres. 2nd ed. Manchester: The Textile Institute, 1975.
[11] Krassig HA. Cellulose structure, accessibility and reactivity. Gordon and Breach, 1993.
[12] Manabe S, Fujioka R. Polym J 1996;28:860.
[13] Lenz J, Schurz J, Wrentschur E. Colloid Polym Sci 1993;271:460.
[14] Heyn J. Appl Phys 1955;26:519.
[15] Grubb DT, Prasad K, Adams W. Polymer 1991;32:1167.
[16] Jakob HF, Fegel D, Tschegg SE, Fratzl P. Macromolecules 1995; 28:8782.
[17] Statton WO. J Polym Sci 1962;58:205.
[18] Perret R, Ruland W. J Appl Cryst 1968;1:308.
[19] Saijo K, Arimoto O, Hashimoto T, Fukuda M, Kawai H. Polymer 1994;35:497.
[20] Crawshaw J, Cameron RE. Polymer 2000;41:4691.
[21] Crawshaw J, Vickers ME, Briggs NP, Cameron RE. Polymer 2000; 41:1873.
[22] Cohen Y, Thomas EL. Macromolecules 1988;21:436.
[23] Wang W, Ruland W, Cohen Y. Acta Polym 1993;44:273.
[24] Ibbett R, Payne J. Patent Application, BP9624538.6, 26th Nov. 1996.
[25] Dettenmaier M. Adv Polym Sci 1983:57.
[26] Glatter O, Kratky O. Small angle X-ray scattering. London: Academic Press, 1982.
[27] Shioya M, Takaku A. J Appl Phys 1985;58:4074.
[28] Perret R, Ruland W. J Appl Cryst 1969;2:209.
[29] Klug HP, Alexander LE. X-ray diffraction procedures. New York: Wiley, 1974.
[30] Bliss N, Bordas J, Fell BD, Harris NW, Helsby WI, Mant GR, Smith W, Towns-Andrews E. Rev Sci Instrum 1995;66(2):1311.
[31] Vonk CG. J Appl Cryst 1975;8:340.
[32] Kolpak FJ, Blackwell J. Macromolecules 1976;9:273.
[33] Janosi A. Z Phys B: Condens Matter 1986;63:375.
[34] Schurz J, Lenz J, Wrentschur E. Die Angewandte Makrolekulare Chemie 1995;229:175.